Combining Theory and Experiment for Multitechnique Characterization of Activated CO_2 on Transition Metal Carbide (001) Surfaces

Christian Kunkel,[†] Francesc Viñes,[†,*] Pedro J. Ramírez,[¨] Jose A. Rodriguez,[‡,*] and Francesc Illas[†]

[†] *Departament de Ciència dels Materials i Química Fisica & Institut de Química Teòrica i Computacional (IQTCUB), Universitat de Barcelona, Martí i Franqués 1-11, 08028 Barcelona, Spain.*

[¨] *Facultad de Ciencias, Universidad Central de Venezuela, Caracas 1020-A, Venezuela.*

[‡] *Chemistry Department, Brookhaven National Laboratory, Upton, NY 11973, USA.*

ABSTRACT

Early transition metal carbides (TMC; TM = Ti, Zr, Hf, V, Nb, Ta, Mo) with face-centered cubic crystallographic structure have emerged as promising materials for CO_2 capture and activation. Density functional theory (DFT) calculations using the Perdew-Burke-Ernzerhof exchange-correlation functional evidence charge transfer from the TMC surface to CO_2 on the two possible adsorption sites –namely MMC and TopC–, and the electronic structure and binding strength differences are discussed. Further, the suitability of multiple experimental techniques with respect to (1) adsorbed CO_2 recognition and (2) MMC/TopC adsorption distinction is assessed from extensive DFT simulations. Results show that ultraviolet photoemission spectroscopies (UPS), work function changes, core level X-ray photoemission spectroscopy (XPS), and changes in linear optical properties could well allow for adsorbed CO_2 detection. Only infrared (IR) spectra and scanning tunnelling microscopy (STM) seem to additionally allow for MMC/TopC adsorption site distinction. These findings are confirmed with experimental XPS measurements, demonstrating CO_2 binding on single crystal (001) surfaces of TiC, ZrC, and VC. The experiments also help resolving ambiguities for VC, where CO_2 activation was unexpected due to low adsorption energy, but could be related to kinetic trapping involving a desorption barrier. With a wealth of data reported and direct experimental evidence provided, this study aims to motivate further basic surface science experiments on an interesting case of CO_2 activating materials, allowing also for a benchmark of employed theoretical models.

* Corresponding authors: francesc.vines@ub.edu, rodrigez@bnl.gov

1. INTRODUCTION

The surface chemistry of CO_2 is an active field of research,[1–3] largely motivated by an urgent need for efficient CO_2 capturing materials. Availability of such materials would facilitate the implementation of technologies for CO_2 capture and storage[4,5] (CCS) or its conversion to value added chemicals, *i.e.* CO_2 capture and usage (CCU). Such routes are ultimately promising for climate change mitigation[6] and worldwide ocean acidification. Still, a relatively high adsorption energy is needed for CO_2 to be captured by a materials surface, only encountered on some privileged materials[1–3] due to the high stability of CO_2 molecules. Moreover, moderate to strong CO_2 adsorption often involves a significant activation, a process requiring charge transfer from the substrate,[1] leading then to weakened C-O bonds, and resulting in a concomitant molecular bending.

As a versatile class of economic materials, transition metal carbides (TMCs)[7,8] have recently proven interesting for CO_2 activation:[9] Results from density functional theory (DFT) based calculations showed the high potential of molybdenum carbides to strongly activate CO_2 on different stable surfaces.[10–13] In fact, experiments on different molybdenum carbide phases[10,13–15] indicate CO_2 dissociation at room temperature, as well as catalytic activity for CO_2 hydrogenation at elevated temperatures, thus indirectly implying the formation of an activated CO_2 moiety. Especially the high CO selectivity and conversion in CO_2 hydrogenation over hexagonal α-Mo_2C powder catalysts is remarkable in the light of practical applications.[13]

Aside from molybdenum carbide, other carbides received less attention, but DFT based calculations on TiC[16] and WC[17] also showed their potential for CO_2 activation. In fact, catalytic tests on TiC, WC, ZrC, NbC, and TaC show CO_2 hydrogenation activity on the respective carbide powders, although with lower conversion compared to Mo_2C.[15] With this promising catalytic activity in mind, a recent comparative DFT study on the most stable (001) surfaces of rocksalt crystal structure and non-magnetic character TiC, ZrC, HfC (group 4), NbC, TaC (group 5), and δ-MoC (group 6) reported strong CO_2 adsorption and activation.[18] In more detail, strength of CO_2 activation was found to vary depending on the transition metal, but always possible on two different adsorption sites exposed on the (001) surface, either in a three-fold hollow position neighboring two metal and one carbon surface metal atom (MMC) or on top of a surface C atom (TopC).

The above mentioned studies demonstrate the potential of TMCs for CO_2 activation, but, apart from evidence coming from DFT calculations, and the implications from catalytic experiments mentioned above, basic surface science experiments on the interaction of CO_2 with well defined single crystal surfaces are a missing piece in this puzzle, although available

and well summarized for other materials.[1,2,19,20] Such studies could provide a detailed microscopic picture of CO_2 adsorption by characterizing adsorbed moieties, commonly achieved by combining multiple complementary experimental techniques,[19] where we refer to some illustrative textbook studies here.[21–24] Still, when trying to interpret such experimental data, a direct comparison to DFT based predictions is of great aid, see for instance combined studies on CO_2 adsorption on Ni,[25] ZnO,[26] or TiO_2[27,28] surfaces.

Thus, to support and further motivate surface science experiments on CO_2 capture, storage, and activation on these materials, we assess the suitability of different experimental techniques on adsorbed CO_2 recognition by *ab initio* simulations, here approximated by means of periodic DFT calculations. This provides extensive data for an interpretation of experimental results. Based on our previous study,[18] we provide simulations of work function changes, simulated infrared (IR) spectra, core level X-ray photoemission spectroscopy (XPS), simulated scanning tunneling microscopy (STM) images, and linear optical properties for CO_2 activated on MMC or TopC sites of the TMCs (001) surfaces. Whenever possible, a comparison of simulated and experimental data provided for bare surfaces gives a first hint at accuracy of the computational simulations. This data is expected to allow an unambiguous distinction for complicated cases of adsorbate geometries and, *vice versa*, to provide a benchmark on the theoretical methods in use. Further, XPS experiments carried out herein proof this concept, providing direct evidence for CO_2 binding on single crystal (001) surfaces of TiC, ZrC, and VC.

2. COMPUTATIONAL AND EXPERIMENTAL DETAILS

Briefly, to assess the properties of CO_2 adsorbed on the different TMCs,[18] periodic DFT calculations were carried out, using slab models and optimized surface-adsorbate geometries previously obtained.[18] All calculations were carried out using the Vienna *Ab Initio* Simulation Package – VASP code.[29] The Perdew-Burke-Ernzerhof (PBE)[30] exchange-correlation (xc) functional was chosen and the contribution of dispersive forces on adsorption energies was contemplated by adding the D3 dispersion correction developed by Grimme[31] (PBE-D3). The effect of core electrons on the valence electron density was taken into account through the projected augmented wave (PAW) method of Blöchl,[32] as implemented by Kresse and Joubert.[33] The valence electron density was expanded in a plane wave basis set with a cutoff kinetic energy of 415 eV. Monkhorst-Pack **k**-point schemes[34] of 17×17×17 and 9×9×1 dimensions were used for bulk and surface slab calculations, respectively. Further details on charge density difference (CDD) analysis, local density of states (DOS) calculations, work function changes, simulated IR and STM, core level shifts, and linear optic properties are

provided in the Supporting Information. Note that all models we use describe a low $^1/_8$ monolayer (ML) CO_2 coverage, where coverage is defined as the number of adsorbate molecules with respect to the number of TM atoms exposed on the surface.

The adsorption of CO_2 was studied by means of suitable experiments on TiC, ZrC, and VC (001) surfaces. The experiments were carried out in an ultra-high vacuum (UHV) chamber that had capabilities for XPS and low-energy electron diffraction (LEED). The metal carbide substrates were prepared and cleaned as described in references.[35,36] These generated surfaces had a very good LEED pattern and a carbon/metal ratio in the range of 0.96-0.98. The metal carbide surfaces were exposed to CO_2 at a temperature of 200 K to avoid physisorption of the molecule. Upon heating to 350 K, the CO_2 desorbed from the carbide substrates without any trace of decomposition (*i.e.* the corresponding C 1*s* and O 1*s* spectra were very similar to those measured before adsorption of the CO_2 molecule).

3. RESULTS AND DISCUSSION

3.1. XPS Experiments

We investigated the adsorption of sub-monolayer amounts of CO_2 on TiC, ZrC, and VC (001) surfaces using XPS. The adsorption of the CO_2 molecules was carried out at 200 K, and by 350 K the adsorbate desorbed without any signs of decomposition, see Figure 1 The amount of CO_2 chemisorbed on TiC(001) and ZrC(001), after a dose of 100 Langmuir (L), was close to 0.5 monolayer (ML). In the case of VC(001), the CO_2 coverage was only 0.15-0.2 ML and could be mainly a consequence of interactions with defects or imperfections instead of interaction with flat terraces (see below). For the clean carbides the C 1*s* peak appeared in the range of 281 to 282 eV in good agreement with XPS data previously reported[35-37] The C 1*s* features for adsorbed CO_2 were centered from 285 to 286 eV. This implies a downward shift of ~4 eV with respect to the C 1*s* peak of the carbides. The O 1*s* for adsorbed CO_2 was detected at binding energies between 532 and 533 eV. These XPS results provide direct evidence for CO_2 activation on single crystal (001) surfaces of TiC, ZrC, and VC. We will further compare these results to our theoretical modelling of core-level XPS, see section 3.7.

3.2. CO_2 adsorption strength

The experimental results presented above give direct evidence for CO_2 activation on the TiC, ZrC, VC (001) surfaces. For the cases of TiC and ZrC, this is consistent with findings of our earlier study[18] probing CO_2 activation on seven rocksalt crystal structure TMCs. For an entry point we therefore reproduce the adsorption energies on MMC and TopC sites, see Table 1. The adsorption energies range between -0.41 and -1.42 eV for the six

TMCs (TM = Ti, Zr, Hf, Nb, Ta, Mo) at the PBE-level, depending on the TMC and specific adsorption site. Inclusion of dispersive forces at the PBE-D3 level predicts slightly more stable minima by 0.21‑0.32 eV. Thus, in addition to TiC and ZrC, four other investigated carbides, namely HfC, NbC, TaC and δ-MoC are also expected to activate CO_2 well.[18] For illustrative purposes, the stable MMC and TopC adsorption geometries of bent (activated) CO_2 are also depicted in Figure 2, here restricted to the case of TiC (001), while being similar for all the carbides, see discussion below.

The case of VC has to be discussed apart. Here, CO_2 activation on MMC and TopC sites seems unfavorable leading to adsorption energies of +0.11 and +0.25 eV, respectively; physisorption being the most stable adsorption mode with a PBE adsorption energy of -0.05 eV. Inclusion of dispersive forces (PBE-D3) renders CO_2 adsorption slightly favorable with adsorption energies of -0.19 and -0.04 eV for MMC and TopC sites, respectively, still physisorption remains more stable (-0.28 eV). CO_2 activation on this material –as evidenced in XPS experiments– seems then surprising at first, but can be explained by a kinetic trapping effect. At the temperature used in the XPS experiments for dosing the molecule (200 K), a desorption barrier of 0.43 eV found from a computed height profile, see Figure 3, could effectively hinder activated CO_2 from leaving the catalyst surface. Additional factors such as defects or C vacancies might favorably contribute to CO_2 binding, although here they are not contemplated.

It still remains noticeable how CO_2 activation on VC is only mildly favorable, whereas TiC and NbC carbides –direct neighbor carbides in the periodic table– activate CO_2 in a highly favored way. The effect can however be understood by decomposing the overall adsorption energy into contributions arising from cost due to geometry changes on (1) the surfaces active sites, and (2) in the CO_2 molecule going together with (3) an attachment energy arising from interaction of both systems at the final geometry. Results given in Table 2 show that the three contemplated TMCs indeed interact strongly with CO_2, leading to highly favored attachment energies (3), while induced geometry changes (1) and (2) counteract this to a differing extent. Especially for VC, attachment energy (3) is almost cancelled by geometry changes (1) and (2). Still, the interaction between surface and CO_2 is distinct and seems similar to other TMCs, making the occurrence of the metastable MMC adsorption state and the given desorption barrier understandable.

Turning back to adsorbate geometry, see Figure 2, MMC and TopC adsorption slightly differ in their relative orientation against the surface with CO_2 being inclined in an MMC hollow adsorption, while TopC CO_2 is oriented perpendicular over a long bridged adsorption mode. Still, the bonding principles seem rather similar, concerning C↔C and metal↔O

interactions between CO_2 and surface sites, to what has been described before.[10,18] We suspect that such similarity could make a clear experimental distinction between these structures difficult, as rather similar electronic properties are likely involved. To ascertain this assumption, we in the following briefly analyze several electronic structure descriptors and next turn to a discussion of experimental techniques that could allow for identification of activated CO_2 and for a distinction between MMC and TopC adsorption.

3.3. Electronic structure analysis

To confirm that a charge transfer from the surface to CO_2 leads to activation and a concomitant bending of the adsorbed molecule, a Bader charge-analysis[38] has been carried out. Results in Table 1 show that adsorbed CO_2 is highly activated, receiving a considerable amount of charge ΔQ of around -0.7 and -1.1 *e* over all cases. The involved charge redistribution can be analyzed in more detail from the CDD plots.

We here focus on the illustrative case of TiC (001) only, see Figure 4a. Adsorption at MMC and TopC sites differs already on first sight. Still, a strong redistribution is obvious with common principles applying for both: The transferred charge largely accumulates between surface carbon and the CO_2 carbon atom, indicative of a covalent C–C bonding. A further significant gain of charge density is found at oxygen atoms; a polarization towards Ti atoms is indicative of electrostatic metal↔O interaction. Note that this binding can be rationalized with surface carbon and titanium atoms of the TiC (001) surface being negatively and positively charges, respectively.[39] Thus these centers favorably interact with the Lewis acidic and basic carbon and oxygen atoms of CO_2.[20]

Charge depletion is visible in areas at the surface, indicative of net charge transfer to the adsorbate, although most obvious is depletion in the C–O bonding regions, indicating that net charge transfer from the surface induces a weakening of bonds. The electron localization function (ELF) allows for an intuitive analysis chemical bonding in the CO_2-surface adsorption complex, see Figure 4b. In agreement with the interpretation from CDD, electron pair density between surface carbon and the CO_2 carbon atom evidences the newly formed covalent bond between adsorbate and surface. Note here, that projected densities of states are provided below, adding further information to the discussion of electronic structure.

3.4. Ultraviolet spectroscopy

Ultraviolet Photoemission Spectroscopies (UPS) have been conveniently used to deduce information about molecular adsorbates on surfaces.[40] For the case of CO_2 adsorption, studies for Fe,[24,41,42] Ni,[43] W,[44] $SrTiO_3$,[45] and Fe_3O_4[22] surfaces provide illustrative examples. In more detail, experimental conditions under which CO_2 is activated[41,43] can be distinguished

from such cases where CO_2 is only molecularly physisorbed.[22] This is possible by analysis of the different peak patterns for CO_2 activation and physisorption in the measured valence band energy region. Interpretation of such peak pattern based can be greatly aided by first principles calculations[41,43–45], *e.g.* by comparison to a systems density of states (DOS), assuming final state effects on energy levels to be negligible.[44] We therefore here provide the local density of states of the systems of interest, discussing first the representative example of CO_2 adsorption on TiC (001), see Figure 5. Note that we focus here on CO_2 induced changes, a thorough discussion of the bare surface DOS is provided in Ref. 39. Red traces in Figure 5 specify the contribution of CO_2 related states. Labels were assigned by visual inspection of the partial charge density in the respective energy range.

For physisorption on the bare surface, the DOS can merely be understood as a combination of bare surface states and states of gas-phase CO_2 in $D_{\infty h}$ symmetry, as was expected. CO_2 activation on MMC or TopC changes this situation distinctly: The wealth of CO_2 related states are then better understandable by looking at the states of a bent CO_2 in gas-phase of C_{2v} symmetry, reported in Figure 5 as well. A significant energetic shift relative to the respective gas-phase orbitals is however seen for the $6a_1/1b_1$ labeled orbitals. Note that this labeling was used as unambiguous assignment of $6a_1$ and $1b_1$ is difficult, due to significant hybridization of these orbitals with surface states. This hybridization serves well as an explanation for the strong and covalent bonding of CO_2 to the surface discussed above. Further, the antibonding $6a_1$ orbital is now populated in the adsorbed CO_2, ultimately the cause for weakened and elongated C-O bonds,[1,19] illustrating nicely the concept of adsorption induced activation.

The DOS for the other studied cases than CO_2 are given in Figure S2 in the Supporting Information. For all cases appearing peaks in the DOS are distinctly different for CO_2 physisorption and activation. UPS should then give good indications for CO_2 activation on the studied systems; it should be noted, however, that peak energy differences between MMC and TopC adsorption are quite small for all cases; a distinction of adsorption sites therefore would be hampered by experimental resolution.

3.5. Work function changes

In experimental and theoretical works considering CO_2 activation on Ni[25,43] and Co,[46,47] a ~1.0 eV increase in the work function was induced when exposing the bare substrate to CO_2. Such an increase is often related with charge transfer from the substrate to CO_2 and by analogy is expectable from CO_2 adsorption on TMC (001) surfaces as well. A mere focus

on charge transfer however oversimplifies the picture, given that a strong dependence on the substrate is well known.[48]

Therefore, to clarify the situation for TMC (001) surfaces, the difference between naked and CO_2 covered surface ($\Delta\phi = \phi_{S/CO_2} - \phi_S$) has been calculated and is reported in Table 1. CO_2 adsorption thereby induces considerable changes, with $\Delta\phi$ ranging between 0.8-1.2 eV for the different cases at the considered coverage. Adsorption on ZrC (001) proves an exception here, with $\Delta\phi$ on the order of 0.5 eV only, yet in all cases charge transfer to CO_2 could explain this change. Note aside that physisorption on TiC, VC, and δ-MoC (001) induced no considerable work function changes and has therefore been omitted for all cases. Work function changes are therefore a convenient indication of CO_2 activation on the studied systems; it should be noted, however, that differences in $\Delta\phi$ between MMC and TopC adsorption are negligible for all cases, making a distinction difficult. Present ϕ_S estimates, found in Table S1 in the Supporting Information, well correlate with those of Viñes *et al.*,[39] obtained using the Perdew-Wang (PW91) exchange-correlation functional.[49]

3.6. Vibrational frequencies

Vibrational frequencies of CO_2 on surfaces can be distinguished from experimental techniques such as high resolution electron energy loss spectroscopy (HREELS)[25,26] or by methods based on IR spectroscopy, see *e.g.* Refs. 13, 28. Especially, these references show how a combination of DFT predicted vibrational frequencies an experiment offers a clear cut interpretation of these spectra. Therefore, to help in a future peak assignment for CO_2 adsorption on the TiC (001) surface, Figure 6 provides its simulated IR spectra.

In more detail, Figure 6 shows the normal mode frequencies for MMC and TopC adsorption. From visual inspection these frequencies ν_{as} and ν_s belong to the asymmetric and symmetric stretch modes of the bent CO_2 molecule, respectively. Clearly, results indicate a large deviation of ν_{as} and ν_s values between MMC or TopC adsorption and the respective gas-phase CO_2 values of 2371 and 1323 cm^{-1}. This difference is understandable from the charge-transfer to adsorbed CO_2 and the concomitant weakening of C-O bonds. More importantly, MMC and TopC adsorption could be distinguishable in experiments, with respective ν_{as} values of 1454 and 1514 cm^{-1} differing by 60 cm^{-1} between the two cases and ν_s values of 1193 and 1222 cm^{-1} differing by 29 cm^{-1}. For an experimental detection, the symmetric stretch however seems better suited given its higher predicted relative intensity. For CO_2 adsorption on all other carbides similar observations can be made, while the differences between MMC and TopC can in some cases be even more pronounced, see *e.g.* the case of

adsorption on TaC. We refer to Figure S1 of the Supporting Information for an overview of the remaining cases.

3.7. Simulated Core-level XPS

To interpret XPS spectra of each TMC + CO_2 system, three different CO_2 adsorption situations seem interesting from a theoretical point of view: Signatures for activated CO_2 adsorbed on *i)* MMC and *ii)* TopC sites might have to be distinguished. Additionally, *iii)* CO_2 physisorption possibly occurs at low temperatures of measurement. Adding to that, since physisorption induces little alteration in CO_2 electronic structure, case *iii)* also serves the purpose to provide a reference for gas phase CO_2. Therefore, calculated core level binding energy shifts (CLBES) values obtained in the initial state model (IS) as well as the Janak-Slater model (JS) are provided in the following for cases *i-iii)*. Note in passing by that computed core levels binding energies are here listed as negative energies, highlighting such as being bound states, at variance with the common experimental fashion, where binding energies are shown positive, in accordance with the promoted unbound electrons.

Before turning to CO_2 adsorption however, a qualitative evaluation of the method performance is interesting for the bare TMC (001) surfaces, possible here by comparing to high-quality experimental data. Surface CLBES for C 1*s* are provided for all carbides in Table S1 of the Supporting Information, calculated from the binding energy difference of a first and third surface layers carbon atoms in the slab surface model. Direct comparison shows the experimental surface CLBES values of 0.26, 0.23, and 0.33 eV for TiC,[50] ZrC,[51] and VC[52] surfaces to be reproduced within ~0.1 eV by the corresponding JS values of 0.25, 0.31 and 0.23 eV. IS values of 0.06, 0.09 and 0.07 eV slightly underestimate these surface CLBES, but more importantly, both models reliably point in the right direction.

Addressing now the CLBES expected for CO_2 adsorption, we first discuss the case of the C 1*s* of CO_2 in the different cases *i-iii)*. These CLBES are given and discussed with reference to a surface carbon atom, a viable choice in an UHV experiment as shown in Figure 1. Note that, in this way, the CLBEs reported are in fact core level binding energy shifts. Results for all TMCs are listed in Table 3 and, for a short discussion we focus on CO_2 adsorption on TiC (001), while conclusions are largely transferable to the other systems.

Looking first at IS model predictions, a physisorbed CO_2 with a CLBES of -5.15 eV would then give rise to a feature clearly distinguishable from those arising from activated CO_2 adsorbed on MMC or TopC sites: For these latter cases, CLBES of -3.75 eV on MMC and -3.69 eV on TopC are found. As expected from the charge transfer arguments discussed above,

the binding energy then diminishes in comparison to physisorbed and largely unperturbed CO_2. Likely the signals arising from MMC and TopC adsorption would be hardly distinguishable among themselves given the small CLS difference of 0.06 eV only. The JS model provides similar conclusions. A CLBES for physisorbed CO_2 of -8.68 eV is found, largely differing from values of -5.45 and -5.54 eV for MMC and TopC adsorption; again signals arising from the latter sites are likely indistinguishable.

Thus, qualitatively similar conclusions are found from both models, still differences between IS and JS predictions are apparent, *e.g.* for MMC adsorption, CLBES differ by 1.70 eV. Clearly, the final state effects incorporated in the JS model lead to a higher CO_2 C 1*s* binding energy, not captured from solely considering initial state effects in the IS model, nevertheless the more accurate model is best chosen to carry out comparison to experiment. The experiments presented in Figure 1 imply a shift of ~4 eV with respect to the C 1s peak of TiC, ZrC and VC. This shift is in reasonable semi-quantitative agreement with IS model predictions for MMC (TopC) adsorption ranging -2.58 (-2.61) to -3.98 (-3.91) eV between the three experimentally investigated carbides. Clearly, the JS here seems to overestimate the shifts with the predicted values in the range of -4.06 (-4.25) to -5.66 (-5.69) eV. Note, that, given the temperature of measurement (200 K), physisorption could already be discarded as a cause for the experimental feature in the XPS of Figure 1. Similar conclusion emerge from the calculated CLBEs in the range of -4.13 (-7.51) to -6.06 (-8.48) eV as predicted by the IS (JS) model. Let us move now to the O 1*s* CLBES of CO_2 in the different cases *i-iii)*. Since referencing to a surface related signal is here not possible, we instead use the O 1*s* level of physisorbed CO_2. Results are listed in Table 4 and we again turn to CO_2 adsorption on TiC (001). IS model predictions yield a positive CLBES of 2.51 and 2.49 eV for MMC and Top C adsorption, expected from charge transfer from the surface, although again the small difference likely makes signals indistinguishable among them. JS model calculations lead to positive CLBES as well, still values of 5.18 and 5.20 eV differ from IS model predictions, due to the inclusion of final state effects.

3.8. Simulation of STM images

STM has proven powerful to unambiguously identify CO_2 adsorption geometries on well-defined surfaces, especially when compared to DFT predicted adsorption minima and the derived STM images. Experimental studies on Au nanoclusters,[53] as well as combined studies on Ni (110)[54] and TiO_2 (110)[27] provide illustrative examples. Here, we provide simulated STM images of the bare TMC surfaces, and the ones derived from CO_2 adsorption on MMC and TopC adsorption geometries. For the exemplifying case of TiC (001), images are given in

Figure 7 and will be discussed in the following; for all other cases we refer to Figure S3 of the Supporting Information.

To produce well-resolved simulated STM images for each system, different pairs of bias voltages and tunneling currents were systematically tested, arriving at the optimum values given below each image in Figure 7. For most cases, to image bare surfaces a simulated tip bias voltage of ± 0.1 V proved valuable at a constant current of ~1.0 nA. In fact rather similar conditions were used in STM experiments on NbC (001)[55] and $VC_{0.8}$ (111),[56] noting that a reversal of bias remained without a noticeable influence on image appearance, as we can affirm from simulated images in most cases. As expected, the TiC (001) bare surface then exhibits the expected ordered pattern with C (Ti) atoms appearing bright (dark).

Simulated images (for ±1.0 V and 1.0 nA) for CO_2 adsorption in both cases clearly show this adsorbed molecule as a bright species, surrounded by dark areas, likely a consequence of charge transfer to the adsorbate. A note of caution however, is that in this formalism, a STM tip is modeled as an infinitely small point source leading to high resolution, possibly diminishing under experimental conditions. Nevertheless, according to these predictions, MMC and TopC adsorption modes of CO_2 would be distinguishable by appearance, given they display one or two symmetry planes, respectively. Determining the lattice directions in an uncovered surface area could simplify the assignment further, given the differing relative orientations between MMC and TopC adsorption.

3.9. Linear optical properties

Adsorption of molecules on a materials surface can introduce changes in the linear optical response.[57,58] In more detail, changes in the materials dielectric functions are then induced by adsorption, leading to respective changes *e.g.* directly measurable by absorption-, reflectance- or in electron energy-loss spectroscopy. To predict changes expected from CO_2 adsorption on the TMC (001) surfaces, we here evaluate the respective linear dielectric response of each model neglecting local field effects.[59] Although formally not fully justified, such DFT based approaches have been widely successful for metallic systems, providing qualitative and even up to quantitative predictions of optical properties, see *e.g.* Refs. 57,60,61.

Few studies have investigated the optical properties of bare TMC (001) surface at this level of theory. Nevertheless, experimental data are available for near stoichiometric samples of TiC, VC, and NbC,[62] and we provide a comparison to our theoretical predictions for the naked surfaces first. In Figure 8, reflectance spectra R(ω) are reported for these three TMCs, for loss functions L(ω) we refer to Figures S4 of the Supporting Information. Although the

calculated spectra are unbroadened and thus exhibit significantly more features, they qualitatively reproduce the trends and main features apparent from the experimental curves quite well. Slight deviations in the low-energy region are visible, and these parts of the spectrum should be interpreted with caution. Possibly, inclusion of intraband contributions[57] and local field effects could improve the description in this energy range. It is also notable that experimental reflectance spectra show overall higher reflectance than reproduced by calculations on surface slabs, while bulk model predictions often agree with experimental values. Including a larger number of layers in the slab model could therefore remedy this behavior.[59] Note however, that the obtainable spectra heavily depend on sample preparation. Still, in the following, we focus on the relative changes induced upon CO_2 adsorption, thus keeping the model.

Knowing that the present theoretical model performs reasonably well, qualitatively predicting the linear optical properties of the three bulk carbides, we now assess changes induced upon CO_2 adsorption, focusing here first on TiC (001). In Figure 9, the predicted changes for different optical properties are given: Over the whole energy range, reflectance $R(\omega)$ and absorption coefficient $\alpha(\omega)$ are expected to rise when CO_2 gets adsorbed, while for the energy loss function $L(\omega)$, this holds true above 16.8 eV. The refractive index $n(\omega)$ and extinction coefficient $k(\omega)$ are mainly influenced by CO_2 adsorption below 5.0 eV. On this basis it is suggested, that CO_2 activation can be demonstrated from changes in measured optical properties of the material. MMC and TopC adsorption, however, are likely indistinguishable, as induced changes are similar for both cases in the realm of model validity. An overview for CO_2 adsorption on other TMCs is provided by Figures S4-S9 of the Supporting Information.

4. SUMMARY AND CONCLUSIONS

In summary, a combined theoretical and experimental study of CO_2 adsorption and detection on the stable (001) surfaces of different transition metal carbides (TMCs) is here reported. In a first-principles based multitechnique exhaustive study using DFT calculations at the PBE level, extensive data for CO_2 adsorption on TMCs (TM = Ti, Zr, Hf, Nb, Ta, Mo) is presented, pointing out how CO_2 activation could be evidenced from different experimental techniques.

Electronic structure analysis carried out on TiC for two competitive adsorption sites (MMC and TopC) evidences charge transfer from the surface to be the underlying mechanism for CO_2 activation. With similar bonding mechanism, but differing bonding strength, electronic structures and adsorbate symmetries, a distinction between adsorption at MMC and TopC sites seems possible through certain experimental techniques, while others might only

allow for a detection of activated CO_2 in general: A significant increase in work function is predicted for TMCs (TM = Ti, Zr, Hf, Nb, Ta, Mo) upon CO_2 exposure, in line with charge transfer from the surface, while a distinction seems difficult on this basis. Vibrational spectroscopy seems better suited: Here, the vibrational signatures of activated CO_2 differ strongly from the gas-phase counterpart, and differences of 60 cm^{-1} and 29 cm^{-1} in asymmetric and symmetric stretching frequencies of MMC and TopC adsorbed CO_2 likely allow for a distinction. Further techniques under investigation were UPS, where in principle activated CO_2 orbitals are detectable, yet no allowing distinction between adsorption at MMC and TopC sites. A change in linear optical properties is further predicted upon CO_2 exposure, still MMC and TopC adsorption are likely indistinguishable. STM however could further provide a means to distinguish MMC and TopC adsorption with the differing adsorbate symmetry being reflected in the simulated STM images. The core level binding energies as extracted from IS and JS approximations on chemisorbed CO_2 reveal a shift indicative of CO_2 activation, in accordance with experiments, although the resolution is too low to distinguish among adsorptive conformations.

With a wealth of simulations carried out on an important example, we expect the present study to provide also a concise exploration into multitechnique simulation of surface adsorption by means of state-of-the-art DFT. A proof of this concept is provided by experimental results for transition metal carbides TiC, ZrC, and VC, lending direct first significant evidence of the previously computationally predicted CO_2 activation on the (001) surfaces.

ASSOCIATED CONTENT

Supporting Information: The Supporting Information is available free of charge on the ACS Publications website at DOI: XXXXXXXXXXX. Further computational details, information on the calculation of charge density differences (CDD), work function changes, the simulation of i) IR spectra, ii) core level binding energies, iii) STM images, iv) linear optical properties. Computed work functions for bare and CO_2 adsorbed surfaces. Complete set of simulated IR spectra, LDOS, STM images, and linear optical properties.

ACKNOWLEDGEMENTS

This work was supported by Spanish *Ministerio de Economía y Competitividad* (MEC) CTQ2015-64618-R grant, *Generalitat de Catalunya* grants 2014SGR97 and XRQTC, and EU H2020 NOMAD project No 676580. F.V. thanks Spanish MEC for a *Ramón y Cajal* research contract (RYC-2012-10129). F.I. acknowledges additional support from the 2015 ICREA Academia Award for Excellence in Research. The experimental studies carried out at Brookhaven National Laboratory were supported by the US Department of Energy, Chemical Sciences Division (DE-SC0012704). The work of P.J.R. was in part financed by research grants of BID and Metallurgia.

Table 1. Adsorption energies (E_{ads} in eV), net charge transfer ΔQ (in e) and induced work function change Δϕ (in eV) for CO_2 adsorption on the different TMC (001) surfaces. Adsorption energies at the PBE (-D3) level of theory have been reproduced from Ref. 18 and include zero point energy (ZPE) contributions

(001) Surface	Site	E_{ads}	ΔQ (CO_2)	Δϕ
TiC	MMC	-0.55 (-0.81)	-0.87	1.0
	TopC	-0.57 (-0.83)	-0.74	1.1
ZrC	MMC	-1.34 (-1.56)	-1.00	0.5
	TopC	-1.39 (-1.60)	-1.10	0.5
HfC	MMC	-1.38 (-1.62)	-1.00	1.2
	TopC	-1.42 (-1.65)	-1.10	1.3
VC	MMC	+0.11(-0.19)	-0.84	1.2
	TopC	+0.25 (-0.04)	-0.78	1.3
NbC	MMC	-0.59 (-0.87)	-0.95	1.1
	TopC	-0.41 (-0.70)	-0.82	1.1
TaC	MMC	-0.95 (-1.21)	-1.09	1.2
	TopC	-0.67 (-0.94)	-1.00	1.2
δ-MoC	MMC	-0.89 (-1.20)	-0.83	0.8
	TopC	-0.71 (-1.03)	-0.98	0.9

* Physisorption is most stable with E_{ads} of -0.05 (-0.28) eV.

Table 2. Energetic contributions (in eV) to CO_2 adsorption on three TMC (001) surfaces, as described in the text. All energies obtained at the PBE-D3 level of theory.

(001) Surface	Surface reorg.	Adsorbate reorg.	Attachment energy (3)	E_{ads}
TiC	+0.46	+2.98	-4.30	-0.85
VC	+0.75	+2.91	-3.88	-0.22
NbC	+0.91	+3.25	-5.06	-0.90

Table 3. Calculated initial state (IS) and final Janak-Slater (JS) C 1*s* core level shifts (in eV) for CO_2 adsorbed on the different TMC (001) surface slabs.

Surface	Site	C 1*s* ($\underline{\mathbf{C}}O_2$-$\underline{\mathbf{C}}_s$)	
		IS	**JS**
TiC	Phys.	-5.15	-8.68
	MMC	-3.75	-5.45
	TopC	-3.69	-5.54
ZrC	Phys.	-6.06	-8.48
	MMC	-3.98	-5.66
	TopC	-3.91	-5.69
HfC	Phys.	-6.21	-8.55
	MMC	-4.27	-5.85
	TopC	-4.25	-5.89
VC	Phys.	-4.13	-7.51
	MMC	-2.58	-4.06
	TopC	-2.61	-4.25
NbC	Phys.	-4.89	-7.06
	MMC	-2.69	-4.04
	TopC	-2.78	-4.14
TaC	Phys	-5.16	-6.91
	MMC	-3.02	-4.02
	TopC	-3.10	-4.19
δ-MoC	Phys	-3.54	-7.22
	MMC	-2.12	-3.73
	TopC	-2.09	-3.74

Table 4. Calculated initial state (IS) and final Janak-Slater (JS) O 1*s* core level binding energy shifts (in eV) for CO_2 adsorbed on the different TMC (001) surface slabs.

Surface	Site	O 1*s* C**O**$_2$ (ads-gas)	
		IS	**JS**
TiC	MMC	2.51	5.20
	TopC	2.48	5.18
ZrC	MMC	2.91	4.01
	TopC	3.01	4.06
HfC	MMC	3.02	4.68
	TopC	2.96	4.68
VC	MMC	2.47	5.06
	TopC	2.47	5.09
NbC	MMC	3.07	4.65
	TopC	2.97	4.71
TaC	MMC	2.99	4.28
	TopC	2.92	4.37
δ-MoC	MMC	2.18	4.17
	TopC	2.23	4.41

Figure 1. C 1*s* XPS spectra collected before and after dosing 100 L of CO_2 to ZrC(001) at 200 K with subsequent annealing to 350 K.

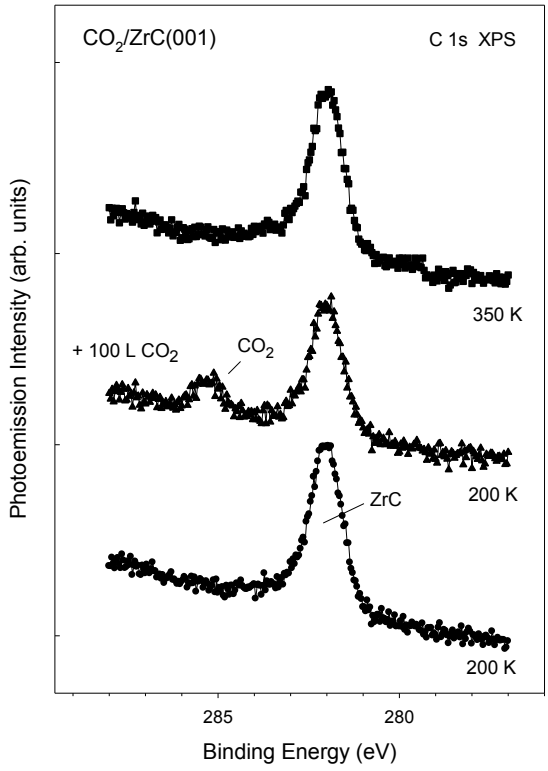

Figure 2. Sketches of CO_2 adsorbed on (a) MMC and (b) TopC sites of the TiC(001) surface slab model. Lighter colour layers were fixed during optimization. For respective side and top views see Ref. 18.

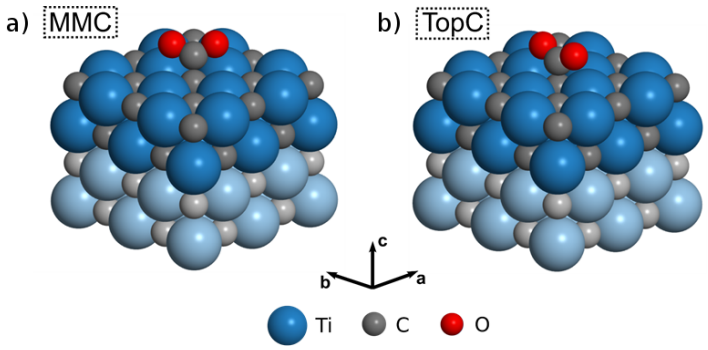

Figure 3. CO_2 adsorption energy height profile above a VC (001) MMC site. Inserted images indicate geometries at stationary points (O: red, V: purple, C: gray), while connecting lines have been introduced for clearness of visualization.

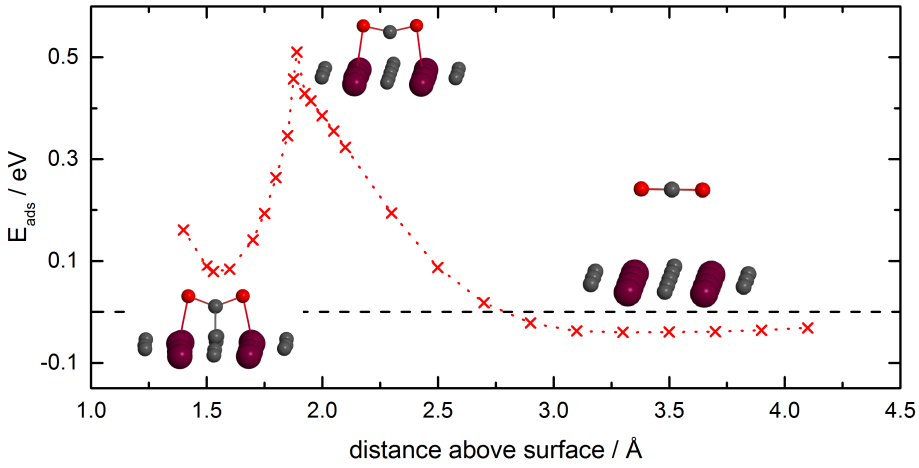

Figure 4. a) CDD for the MMC and TopC site. Yellow (grey) isosurfaces denote areas of charge accumulation (depletion), with isovalues of 0.05 and 0.07 e/Å^3, respectively. **b)** ELF images for MMC and TopC site in the plane of the CO_2 molecule. The probability of finding an electron pair is given by a colour code as indicated. Coloured spheres indicate atom positions, colouring for all atoms as in Figure 1.

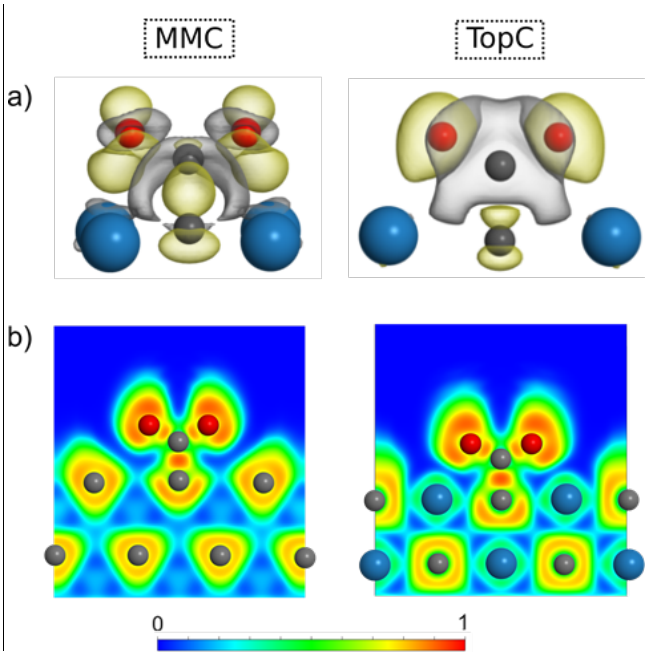

Figure 5. Local density of states (DOS) for CO_2 adsorption on the upper two surface layers of TiC (001). From top to bottom: CO_2 physisorption on TiC (001), CO_2 MMC adsorption on TiC (001), gas-phase CO_2 (neutral, in bent geometry), and CO_2 TopC adsorption on TiC (001). All cases aligned to their respective vacuum levels with a common zero introduced by the Fermi-level of the TiC (001) surface with physisorbed CO_2 (dashed gray line). Dashed vertical blue lines indicate the relative Fermi-levels of all remaining systems. An induced work function change $\Delta\phi$ is indicated, see discussion below.

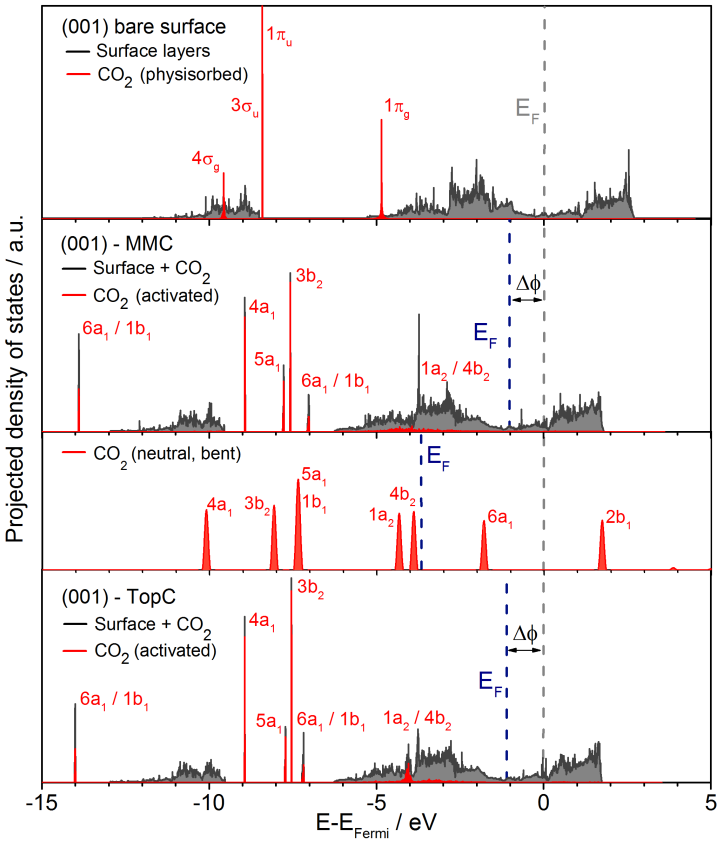

Figure 6. Simulated IR spectra of CO_2 adsorbed on the TiC (001) surface. Peaks are marked with their vibrational frequency (in cm^{-1}). Relative intensities (Rel. int.) of the asymmetric stretch were overall low and have been slightly increased for better visibility.

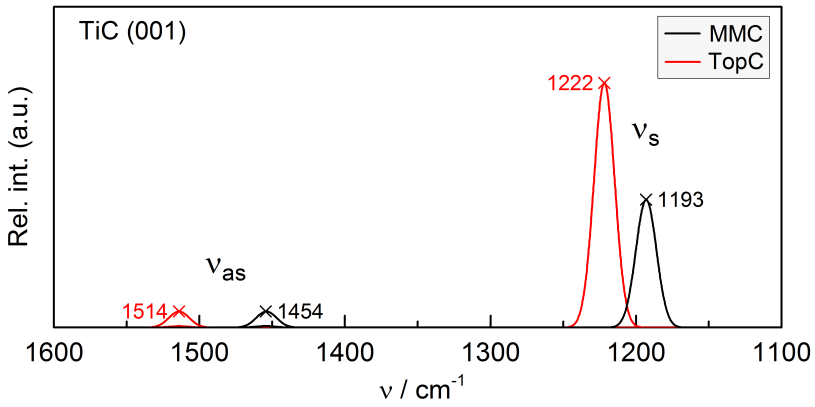

Figure 7. Simulated constant current STM images for bare TiC (001) surface and CO_2 adsorbed on MMC and TopC sites. Simulated conditions of tip bias and current are given below each image. For a better contrast, images have been coloured. Positions of CO_2 carbon (oxygen) atom(s) have been indicated by gray (red) spheres. The given lattice directions are similar in all images.

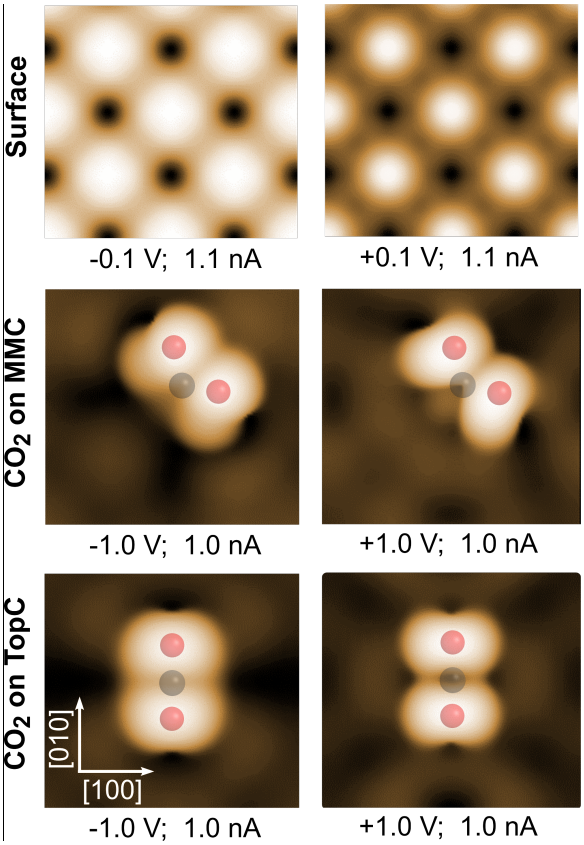

Figure 8. Reflectance spectra for TiC, VC, and NbC in the energy range from 0-30 eV. The experimental spectra have been reproduced from the work of Koide *et al.*[62] for the nearly stoichiometric $TiC_{0.95}$, $VC_{0.86}$, and $NbC_{0.93}$, respectively.

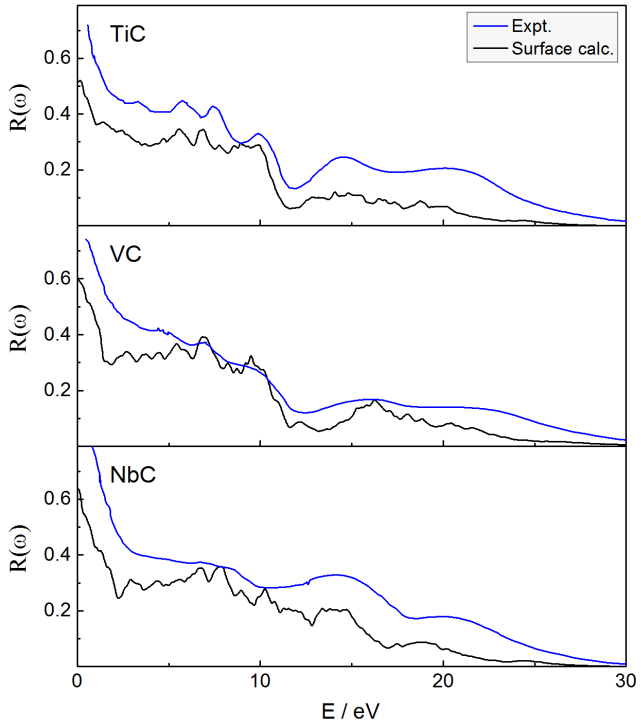

Figure 9. Change of linear optical properties induced by CO_2 adsorption (MMC or TopC) on the TiC (001) surface slab model in the energy range from 0-30 eV. For a definition of the plotted quantities, see text.

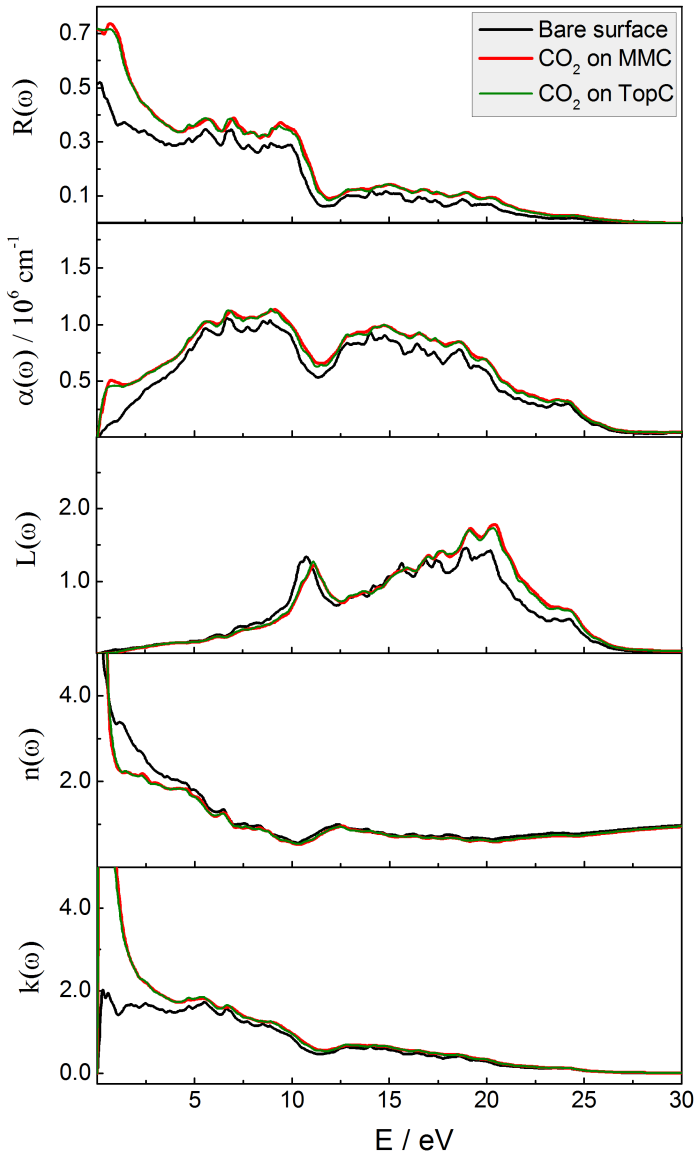

References

(1) Freund, H.; Roberts, M. W. Surface Chemistry of Carbon Dioxide. *Surf. Sci. Rep.* **1996**, *25*, 225–273.

(2) Burghaus, U. Perspective of Carbon Dioxide Chemistry — Adsorption Kinetics and Dynamics of CO_2 on Selected Model Surfaces. Surf. Sci. **2009**, *148*, 212–220.

(3) Taifan, W.; Boily, J.-F.; Baltrusaitis, J. Surface Chemistry of Carbon Dioxide Revisited. *Surf. Sci. Rep.* **2016**, *71*, 595–671.

(4) Espinal, L.; Poster, D. L.; Wong-Ng, W.; Allen, A. J.; Green, M. L. Measurement, Standards, and Data Needs for CO_2 Capture Materials: A Critical Review. *Environ. Sci. Technol.* **2013**, *47*, 11960–11975.

(5) D'Alessandro, D. M.; Smit, B.; Long, J. R. Carbon Dioxide Capture: Prospects for New Materials. *Angew. Chemie - Int. Ed.* **2010**, *49*, 6058–6082.

(6) Edenhofer, O.; Pichs-Madruga, R.; Sokona, Y.; Minx, J. C.; Farahani, E.; Susanne, K.; Seyboth, K.; Adler, A.; Baum, I.; Brunner, S.; et al. *Climate Change 2014: Mitigation of Climate Change*; 2014.

(7) Levy, R. B.; Boudart, M. Platinum-like Behavior of Tungsten Carbide in Surface Catalysis. *Science* **1973**, *181*, 547–549.

(8) Hwu, H. H.; Chen, J. G. Surface Chemistry of Transition Metal Carbides. *Chem. Rev.* **2005**, *105*, 185–212.

(9) Posada-Pérez, S.; Viñes, F.; Rodriguez, J. A.; Illas, F. Fundamentals of Methanol Synthesis on Metal Carbide Based Catalysts: Activation of CO_2 and H_2. *Top. Catal.* **2014**, *58*, 159–173.

(10) Posada-Pérez, S.; Viñes, F.; Ramirez, P. J.; Vidal, A. B.; Rodriguez, J. A.; Illas, F. The Bending Machine: CO_2 Activation and Hydrogenation on δ-MoC(001) and β-Mo2C(001) Surfaces. *Phys. Chem. Chem. Phys.* **2014**, *16*, 14912–14921.

(11) Shi, Y.; Yang, Y.; Li, Y. W.; Jiao, H. Activation Mechanisms of H_2, O_2, H_2O, CO_2, CO, CH_4 and C_2H_x on Metallic $Mo_2C(001)$ as Well as Mo/C Terminated $Mo_2C(101)$ from Density Functional Theory Computations. *Appl. Catal. A Gen.* **2016**, *524*, 223–236.

(12) Ren, J.; Huo, C.-F.; Wang, J.; Cao, Z.; Li, Y.-W.; Jiao, H. Density Functional Theory Study into the Adsorption of CO_2, H and CH_x (x=0–3) as Well as C_2H_4 on α-$Mo_2C(0001)$. *Surf. Sci.* **2006**, *600*, 2329–2337.

(13) Liu, X.; Kunkel, C. R.; Ramirez De La Piscina, P.; Homs, N.; Viñes, F.; Illas, F. Effective and Highly Selective CO Generation from CO_2 Using a Polycrystalline α-Mo_2C Catalyst. *ACS Catal.* **2017**, *7*, 4323–4335.

(14) Porosoff, M. D.; Yang, X.; Boscoboinik, J. A.; Chen, J. G. Molybdenum Carbide as Alternative Catalysts to Precious Metals for Highly Selective Reduction of CO_2 to CO. *Angew. Chemie - Int. Ed.* **2014**, *53*, 6705–6709.

(15) Porosoff, M. D.; Kattel, S.; Li, W.; Liu, P.; Chen, J. G. Identifying Trends and Descriptors for Selective CO_2 Conversion to CO over Transition Metal Carbides. *Chem. Commun.* **2015**, *51*, 6988–6991.

(16) Vidal, A. B.; Feria, L.; Evans, J.; Takahashi, Y.; Liu, P.; Nakamura, K.; Illas, F.; Rodriguez, J. A. CO_2 Activation and Methanol Synthesis on Novel Au/TiC and Cu/TiC Catalysts. *J. Phys. Chem. Lett.* **2012**, *3*, 2275–2280.

(17) Wu, S.; Ho, J. Adsorption, Dissociation, and Hydrogenation of CO_2 on WC (0001) and WC-Co Alloy Surfaces Investigated with Theoretical Calculations. *J. Phys. Chem. C* **2012**, *116*, 13202–13209.

(18) Kunkel, C.; Viñes, F.; Illas, F. Transition Metal Carbides as Novel Materials for CO_2 Capture, Storage, and Activation. *Energy Environ. Sci.* **2016**, *9*, 141–144.

(19) Taifan, W.; Boily, J.-F.; Baltrusaitis, J. Surface Chemistry of Carbon Dioxide Revisited. *Surf. Sci. Rep.* **2016**, *71*, 595–671.

(20) Burghaus, U. Progress in Surface Science Surface Chemistry of CO_2 – Adsorption of Carbon Dioxide on Clean Surfaces at Ultrahigh Vacuum. *Prog. Surf. Sci.* **2014**, *89*, 161–217.

(21) Humblot, V.; Haq, S.; Muryn, C.; Hofer, W. A.; Raval, R. From Local Adsorption Stresses to Chiral Surfaces: (R,R)-Tartaric Acid on Ni(110). *J. Am. Chem. Soc.* **2002**, *124* (3), 503–510.

(22) Pavelec, J.; Hulva, J.; Halwidl, D.; Bliem, R.; Gamba, O.; Jakub, Z.; Brunbauer, F.; Schmid, M.; Diebold, U.; Parkinson, G. S. A Multi-Technique Study of CO_2 Adsorption on Fe_3O_4 Magnetite. *J. Chem. Phys.* **2017**, *146*, 14701.

(23) Setvin, M.; Buchholz, M.; Hou, W.; Zhang, C.; Sto, B.; Hulva, J.; Simschitz, T.; Shi, X.; Pavelec, J.; Parkinson, G. S.; et al. A Multitechnique Study of CO Adsorption on the TiO_2 Anatase (101) Surface. **2015**, *119*, 21044–21052.

(24) Nassir, M. H. Sequential Carbon Oxygen Bond Cleavage in Chemisorption of CO_2 on Fe(100). *J. Vac. Sci. Technol. A* **1993**, *11*, 2104.

(25) Ding, X. Interaction of Carbon Dioxide with Ni (110): A Combined Experimental and Theoretical Study. **2007**, No. 110, 1–12.

(26) Wang, Y.; Kováčik, R.; Meyer, B.; Kotsis, K.; Stodt, D.; Staemmler, V.; Qiu, H.; Traeger, F.; Langenberg, D.; Muhler, M.; et al. CO_2 Activation by ZnO through the Formation of an Unusual Tridentate Surface Carbonate. *Angew. Chem. Int. Ed.* **2007**, *46*, 5624–5627.

(27) Lin, X.; Yoon, Y.; Petrik, N. G.; Li, Z.; Wang, Z.; Glezakou, V.; Kay, B. D.; Lyubinetsky, I.; Kimmel, G. a; Rousseau, R.; et al. Structure and Dynamics of CO_2 on Rutile TiO_2 (110)-1×1. *J. Phys. Chem. C* **2012**, *116*, 26322–26334.

(28) Mino, L.; Spoto, G.; Ferrari, A. M. CO_2 Capture by TiO_2 Anatase Surfaces : A Combined DFT and FTIR Study. *J. Phys. Chem. C* **2014**, *118*, 25016–25026.

(29) Kresse, G.; Furthmüller, J. Efficient Iterative Schemes for Ab Initio Total-Energy Calculations Using a Plane-Wave Basis Set. *Phys. Rev. B* **1996**, *54*, 11169–11186.

(30) Perdew, J. P.; Burke, K.; Ernzerhof, M. Generalized Gradient Approximation Made Simple. *Phys. Rev. Lett.* **1996**, *77*, 3865–3868.

(31) Grimme, S.; Antony, J.; Ehrlich, S.; Krieg, H. A Consistent and Accurate Ab Initio Parametrization of Density Functional Dispersion Correction (DFT-D) for the 94 Elements H-Pu. *J. Chem. Phys.* **2010**, *132*, 154104.

(32) Blöchl, P. E. Projector Augmented-Wave Method. *Phys. Rev. B* **1994**, *50*, 17953–17979.

(33) Kresse, G.; Joubert, D. From Ultrasoft Pseudopotentials to the Projector Augmented-Wave Method. *Phys. Rev. B* **1999**, *59*, 1758–1775.

(34) Monkhorst, H. J.; Pack, J. D. Special Points for Brillouin-Zone Integrations. *Phys. Rev. B* **1976**, *13*, 5188–5192.

(35) Rodriguez, J. A.; Liu, P.; Gomes, J.; Nakamura, K.; Viñes, F.; Sousa, C.; Illas, F. Interaction of Oxygen with ZrC (001) and VC (001): Photoemission and First-Principles Studies. *Phys. Rev. B* **2005**, *72*, 075427.

(36) Rodriguez, J. A.; Liu, P.; Dvorak, J.; Jirsak, T.; Gomes, J.; Takahashi, Y.; Nakamura, K. The Interaction of Oxygen with TiC(001): Photoemission and First-Principles Studies. *J. Chem. Phys.* **2004**, *121*, 465–474.

(37) Balaceanu, M.; Braic, M.; Braic, V.; Vladescu, A.; Negrila, C. C. Surface Chemistry of Plasma Deposited ZrC Hard Coatings. *J. Optoelectr. Adv. Mat.* **2005**, *7*, 2557-2560.

(38) Bader, R. F. W. Atoms in Molecules. In *Encyclopedia of Computational Chemistry*; John Wiley & Sons, Ltd: Chichester, UK, 2002.

(39) Viñes, F.; Sousa, C.; Liu, P.; Rodriguez, J. A.; Illas, F. A Systematic Density Functional Theory Study of the Electronic Structure of Bulk and (001) Surface of Transition-Metals Carbides. *J. Chem. Phys.* **2005**, *122*, 174709.

(40) Freund, H. J.; Neumann, M. Photoemission of Molecular Adsorbates. *Appl. Phys. A* **1988**, *47*, 3–23.

(41) Freund, H. J.; Behner, H.; Bartos, B.; Wedler, G.; Kuhlenbeck, H.; Neumann, M. CO_2 Adsorption and Reaction on Fe(111): An Angle Resolved Photoemission (ARUPS) Study. *Surf. Sci.* **1987**, *180*, 550–564.

(42) Behner, H.; Spiess, W.; Wedler, G.; Borgmann, D. Interaction of Carbon Dioxide with Fe(110), Stepped Fe(100) and Fe(111). *Surf. Sci.* **1986**, *175*, 276–286.

(43) Bartos, B.; Freund, H. J.; Kuhlenbeck, H.; Neumann, M.; Lindner, H.; Müller, K. Adsorption and Reaction of CO_2 and CO_2/O CO-Adsorption on Ni(110): Angle Resolved Photoemission (ARUPS) and Electron Energy Loss (HREELS) Studies. *Surf. Sci.* **1987**, *179*, 59–89.

(44) Viñes, F.; Borodin, A.; Höfft, O.; Kempter, V.; Illas, F. The Interaction of CO_2 with Sodium-Promoted W(011). *Phys. Chem. Chem. Phys.* **2005**, *7*, 3866-3873.

(45) Baniecki, J. D.; Ishii, M.; Kurihara, K.; Yamanaka, K.; Yano, T.; Shinozaki, K.; Imada, T.; Nozaki, K.; Kin, N. Photoemission and Quantum Chemical Study of $SrTiO_3$(001) Surfaces and Their Interaction with CO_2. *Phys. Rev. B - Condens. Matter Mater. Phys.* **2008**, *78* , 1–12.

(46) Frerichs, M.; Schweiger, F. X.; Voigts, F.; Rudenkiy, S.; Maus-Friedrichs, W.; Kempter, V. Interaction of O_2, CO and CO_2 with Co Films. *Surf. Interface Anal.* **2005**, *37*, 633–640.

(47) de la Peña O'Shea, V. A.; González, S.; Illas, F.; Fierro, J. L. G. Evidence for Spontaneous CO_2 Activation on Cobalt Surfaces. *Chem. Phys. Lett.* **2008**, *454*, 262–268.

(48) Migani, A.; Sousa, C.; Illas, F. Chemisorption of Atomic Chlorine on Metal Surfaces and the Interpretation of the Induced Work Function Changes. *Surf. Sci.* **2005**, *574*, 297–305.

(49) Perdew, J. P.; Chevary, J. A.; Vosko, S. H.; Jackson, K. A.; Pederson, M. R.; Singh, D. J.; Fiolhais, C. Atoms, Molecules, Solids, and Surfaces: Applications of the Generalized Gradient Approximation for Exchange and Correlation. *Phys. Rev. B* **1992**, *46*, 6671–6687.

(50) Johansson, L. I.; Johansson, H. I. P.; Håkansson, K. L. Surface-Shifted N 1 *s* and C 1 *s* Levels on the (100) Surface of TiN and TiC. *Phys. Rev. B* **1993**, *48*, 14520–14523.

(51) Håkansson, K. L.; Johansson, H. I. P.; Johansson, L. I. High-Resolution Core-Level Study of ZrC(100) and Its Reaction with Oxygen. *Phys. Rev. B* **1993**, *48*, 2623–2626.

(52) Håkansson, K. L.; Johansson, L. I.; Hammar, M.; Göthelid, M. High-Resolution Core-Level Studies of $VC_{0.80}$ Surfaces. *Phys. Rev. B* **1993**, *47*, 769–774.

(53) Stiehler, C.; Calaza, F.; Schneider, W. D.; Nilius, N.; Freund, H. J. Molecular Adsorption Changes the Quantum Structure of Oxide-Supported Gold Nanoparticles: Chemisorption versus Physisorption. *Phys. Rev. Lett.* **2015**, *115*, 1–5.

(54) Dri, C.; Peronio, A.; Vesselli, E.; Africh, C.; Rizzi, M.; Baldereschi, A.; Peressi, M.; Comelli, G. Imaging and Characterization of Activated CO_2 Species on Ni(110). *Phys. Rev. B - Condens. Matter Mater. Phys.* **2010**, *82*, 1–6.

(55) Tsong, R.; Schmid, M.; Nagl, C.; Varga, P. Scanning Tunneling Microscopy Studies of Niobium Carbide (100) and (110) Surfaces. *Surf. Sci.* **1996**, *366*, 85–92.

(56) Watson, T.; Heights, Y. Characterization of Carbides by Scanning Tunneling Microscopy. *Mater. Sci. Eng. A* **1988**, *106*, 55–63.

(57) Harl, J.; Kresse, G.; Sun, L. D.; Hohage, M.; Zeppenfeld, P. Ab Initio Reflectance Difference Spectra of the Bare and Adsorbate Covered Cu(110) Surfaces. *Phys. Rev. B - Condens. Matter Mater. Phys.* **2007**, *76*, 20–25.

(58) Baghbanpourasl, A.; Schmidt, W. G.; Denk, M.; Cobet, C.; Hohage, M.; Zeppenfeld, P.; Hingerl, K. Water Adsorbate Influence on the Cu(110) Surface Optical Response. *Surf. Sci.* **2015**, *641*, 231–236.

(59) Gajdoš, M.; Hummer, K.; Kresse, G.; Furthmüller, J.; Bechstedt, F. Linear Optical Properties in the Projector-Augmented Wave Methodology. *Phys. Rev. B - Condens. Matter Mater. Phys.* **2006**, *73*, 1–9.

(60) Prytz, Ø.; Løvvik, O. M.; Taftø, J. Comparison of Theoretical and Experimental Dielectric Functions : Electron Energy-Loss Spectroscopy and Density-Functional Calculations on Skutterudites. *Phys. Rev. B* **2006**, *74*, 245109.

(61) Chimata, R. Optical Properties of Materials Calculated from First Principles Theory, Uppsala University, 2010.

(62) Koide, T.; Shidara, T.; Fukutani, H.; Fujimori, A.; Miyahara, T.; Kato, H.; Otani, S.; Ishizawa, Y. Optical Study of the Stoichiometry-Dependent Electronic Structure of TiC_x, VC_x, and NbC_x. *Phys. Rev. B* **1990**, *42*, 4979–4995.

TOC Graphic

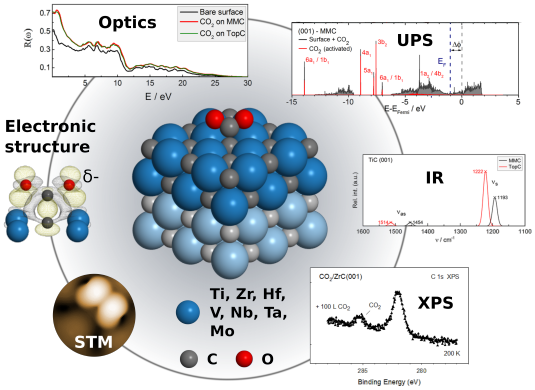
Optics
Bare surface
CO2 on MMC
CO2 on TopC
E / eV
UPS
(001) - MMC
Surface + CO2
CO2 (activated)
Electronic structure
δ-
IR
TiC (001)
MMC
TopC
XPS
CO2/ZrC(001)
C 1s XPS
+ 100 L CO2
200 K
Binding Energy (eV)
STM
Ti, Zr, Hf, V, Nb, Ta, Mo
C
O